Persistent luminescence nanoparticles functionalized by polymers bearing phosphonic acid anchors: synthesis, characterization, and in vivo behaviour

Thomas Lécuyer, Nicolas Bia, Pierre Burckel, Cédric Loubat, Alain Graillot, Johanne Seguin, Yohann Corvis, Jianhua Liu, Lucie Valéro, Daniel Scherman, et al.

Nanoscale

Accepted Manuscript

This article can be cited before page numbers have been issued, to do this please use: T. Lecuyer, N. Bia, P. Burckel, C. Loubat, A. Graillot, J. Seguin, Y. Corvis, J. Liu, L. Valero, D. Scherman, N. Mignet and C. Richard, *Nanoscale*, 2021, DOI: 10.1039/D1NR07114A.

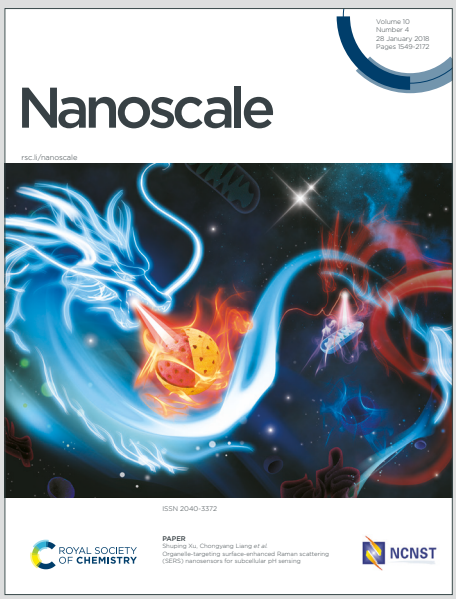

ROYAL SOCIETY OF CHEMISTRY

rsc.li/nanoscale

View Article Online
DOI: 10.1039/D1NR07114A

ARTICLE

Persistent luminescence nanoparticles functionalized by polymers bearing phosphonic acid anchors: synthesis, characterizations, and in vivo behaviour

Received 00th January 20xx,
Accepted 00th January 20xx

DOI: 10.1039/x0xx00000x

Thomas Lécuyer,[a] Nicolas Bia,[b] Pierre Burckel,[c] Cédric Loubat,[b] Alain Graillot,[b] Johanne Seguin,[a] Yohann Corvis,[a] Jianhua Liu,[a] Lucie Valéro,[a] Daniel Scherman,[a] Nathalie Mignet,[a] Cyrille Richard[a]

Optical in vivo imaging has become a widely used technique and is still under development for clinical diagnostics and treatment applications. To further development of the field, researchers have put much effort on the development of inorganic nanoparticles (NPs) as imaging probes. In this trend, our laboratory developed ZnGa1.995O4Cr0.005 (ZGO) nanoparticles, which can emit a bright persistent luminescence signal through the tissue transparency window for dozens of minutes and can be activated in vivo with visible irradiation. These properties confer them unique features, allowing to recover information over a long-time study with in vivo imaging without any background. To target tissues of interest, ZGO must circulate long enough in the blood stream, phenomenon which is limited by the mono nuclear phagocyte system (MPS). Depending on their size, charge and coating, the NPs are sooner or later opsonized and stored into the main organs of the MPS (liver, spleen, lungs). The NPs has therefore to be coated with a hydrophilic polymer to avoid this limitation. To that end, a new functionalization method using two different polyethylene glycol phosphonic acid polymers (a linear one, later named lpPEG and a branched one, later named pPEG) have been studied in this article. The coating has been optimized and characterized in various aqueous media. The comportment of the new functionalized NPs has been investigated in presence of plasmatic proteins, and in vivo biodistribution study has been performed. Among them ZGOpPEG exhibit long circulation time, corresponding to low protein adsorption, while presenting an effective one-step process in aqueous medium with low hydrodynamic diameter increase. This new method is much more advantageous than another strategy we previously reported that used a two-step PEG silane coating performed in an organic solvent (dimethylformamide) for which the final hydrodynamic diameter was twice the initial diameter.

Introduction

Optical *in vivo* imaging has become a widely used technique to identify biological functions and pathologies mechanisms, for both *in vitro* and *in vivo* models, and is under development for clinical diagnostics and treatments.[1] While fluorescent molecules have already reached this achievement, they still possess few disadvantages, such as chemical stability, targeting, or hydrophobicity.[2] To overcome those issues and take advantages of the tremendous benefits of optical imaging, researchers have put efforts on the development of inorganic nanoparticles (NPs) as imaging probes.[3,4] While they are bigger than molecules and proteins, yet smaller than cells, NPs induce new interactions pathways.[5] Their tunability in terms of size, shape, and optical properties, combined to their stability have given them great advantages upon molecular probes.[6]

In this trend, our laboratory recently developed $ZnGa_{1.995}O_4Cr_{0.005}$ nanoparticles or ZGO.[7,8] This material was found to be attractive, both due to its bright near-infrared (λ em = 700 nm) persistent luminescence and its possibility to be activated *in vivo* with visible irradiation. Noteworthy, ZGO nanoparticles can emit a persistent luminescence signal through the tissue transparency window for dozens of minutes, allowing performing *in vivo* imaging without any background. This allows imaging with a high signal to noise ratio, constituting a promising alternative to the actual commercially available optical near infrared probes.[7] More than these unique optical properties, PLNPs have also shown large functionalization capabilities for active targeting.[9] Finally, the absence of *in vitro* and *in vivo* toxicity of ZGO or its constituents has been shown,[10–14] and the degradation of ZGO in artificial lysosomal fluid has been proven.[15] Lately, nanocomposites using ZGO have also been developed for imaging[16] or detection.[17]

Despite these advantages, some fundamental challenges hamper NPs deployment to the clinic, so it is for ZGO.[18] One of these is the uptake by the mononuclear phagocyte system (MPS), in which NPs are rapidly cleared out of the bloodstream to the liver, spleen, lungs or bone marrow, and nonspecific

[a] Université de Paris, CNRS, INSERM, UTCBS, Unité de Technologies Chimiques et Biologiques pour la Santé, Faculté de Pharmacie, 75006 Paris, France
[b] Specific Polymers, ZAC Via Domitia 150 Avenue des Cocardières 34160 Castries (France)
[c] Institut de Physique du Globe de Paris (IPGP), Université de Paris.

Electronic Supplementary Information (ESI) available: [details of any supplementary information available should be included here]. See DOI: 10.1039/x0xx00000x

binding of NPs to nontargeted or healthy areas.[5] This capture is mainly due to the adsorption of plasma proteins facilitating the recognition of the NPs by the macrophages, also known as opsonization.[19] Concerns about NPs toxicity often arise because of this MPS accumulation.[20] Aggregation can lead to NPs entrapment in the liver, lungs, or others due to capillary occlusion. To avoid this uptake, functionalization processes have been developed to passivate the surface of the NPs.[21]

In our laboratory, ZGO were successfully functionalized with polyethylene glycol (PEG), thanks to a two-steps synthesis in organic solvent using silane as anchor group.[22] PEG is inexpensive, versatile and FDA approved for many applications.[23] PEG chains modify the layer in interface with the biological fluids and the nanoparticles, by creating steric effect and annihilating the electrostatic interaction, and therefore reducing the opsonization process, while the unfunctionalized ZGO are opsonized in few minutes.[7] PEG coating has also shown to improve the luminescence properties[24] as well as hemocompability.[14] Nevertheless, this functionalization process doubles the hydrodynamic diameter of the ZGO, which might increase the protein recognition and so affect their biodistribution. Furthermore, silane anchor has shown to be easily degraded in presence of reactive oxygen species (ROS).[25] For these reasons, novel PEG functionalization is needed. In this trend, polyphosphonic acid PEG are new PEG derivatives which have been shown to delay the opsonisation of iron oxide NPs.[26] This statistical poly(methacrylate) based copolymers bearing (i) PEG lateral chains and (ii) phosphonic acid anchoring, allows a new coating strategy and geometry. Phosphonic acid group has already been employed to immobilize organic or organometallic molecules on the surface of metal oxide and has already been used for numerous applications,[27] such as functionalization of quantum dots,[28] IONPs[29], UCNPs[30] (and used as anchoring group for dye-sensitized solar cells.[31] In this work we have evaluated two different PEGylated phosphonic acid polymers with the same chain's length and we have developed a one-step synthesis in aqueous solution leading to NPs with smaller hydrodynamic diameters than the two-steps process described above and used in many studies. A complete characterization has been done and the stability of both polymers coated ZGO in medium used for *in vivo* injection has been investigated. Finally, after determining the number of adsorbed proteins, biodistribution studies in mice has shown a good circulation time (few hours) into the bloodstream, and the results have been compared to our previously reported two-step PEG silane coating strategy. This new functionalization strategy, advantageously performed in aqueous medium, could be a much safer alternative for *in vivo* studies and industrial development.

Results and discussion

Synthesis and characterization

The ZGO nanoparticles have been prepared as previously described, by a two-step's method with first a hydrothermal treatment from the constituting nitrated ions followed by a 5 h calcination at 750°C.[7] This last step confers to the material its persistent luminescence properties, after both UV and near infrared visible light excitation. The nanoparticles were then extracted from the bulk suspension by selective centrifugation after hydroxylation in hydrochloric acid. We finally obtained stable NPs in aqueous solution with a mean hydrodynamic diameter of 80 nm (called ZGOOH). After injection, the ZGOOH NPs are rapidly trapped by the MPS so further functionalization are needed to have a longer circulation time into the bloodstream. To that end PEGylation of the NPs has been investigated,[22] known as an effective and efficient surface modification process for *in vivo* use. A two-step's reaction has previously been optimized, with first the grafting of aminopropyltriethoxysilane (APTES) followed by N-hydroxysuccinimide activated polyethylene glycol (referred as PEG), and both steps were performed in dimethylformamide (DMF) (Fig. S1). Such PEGylated ZGO, or ZGOPEG, were obtained with a mean hydrodynamic diameter of 145 ± 15 nm leading to ~ 5 h circulation time in the bloodstream. Nevertheless, the use of organic solvents as well as the large increase of size let place for improvement.

To do so, we developed herein a new functionalization strategy of ZGO with new copolymer. The Poly(poly(ethylene glycol methacrylate)-stat-dimethyl(methacryoyloxy) phosphonic acid) (poly(PEGMA-stat-MAPC1acid, referred as pPEG), was prepared as reported in the literature.[32] It consists in two ester moieties: one carrying a PEG lateral chain of 5 kDa (red rectangle in Fig. 1.A) and the second a phosphonic acid anchor (blue rectangle in Fig. 1.A). Phosphonic acid is a functional group of interest for many current fields of research that include medicine (solubilization of bioactive compounds, agonist agents), and material sciences (surface chemistry of electrodes, microfluidic devices).[33] To compare its effectiveness, linear PEG polymer with a mono phosphonic acid anchor (referred as lpPEG, Fig. 1.B) and PEG silane (Fig. 1.C), with same PEG chain length, have also been used as controls.

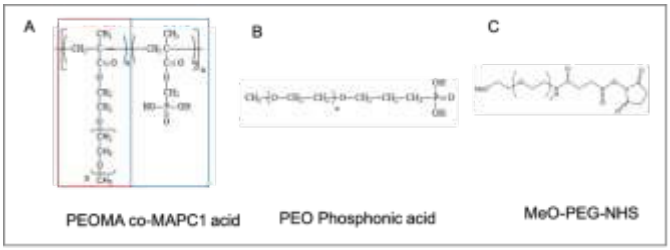

Figure 1: Semi-developed formula of A) Branched pPEG, B) Linear lpPEG and C) PEG. The pPEG has the characteristic to be composed of a repeat of a PEG chain (red rectangle) and a phosphonic acid anchor group (blue rectangle) on each monomer.

Phosphonic acid present two main characteristics to be a valuable anchor group. Firstly, this group possesses two acidic protons, with pKa ranging between 1-3 and 5-8 depending on the attached group,[34] and therefore a good attack site for nucleophilic substitution (SN1 and SN2).[33] Secondly, a strong complexation of divalent cations by the phosphonic acid has been shown.[35,36] The two mechanisms of linkage between the ZGO and the polymers are possible. In both cases a large coating of the surface is expected. Because of the numerous anchors of

the pPEG (n = 13), the polymer can interact with the surface several times, and therefore can "reticulate or attached" all around the NP. This could lead to a denser coating and therefore to a lower protein adsorption.

Functionalization of ZGO by pPEG and lpPEG has been performed in aqueous solution. The influence of several parameters such as the reaction time, the ZGO to polymer mass ratio, or the temperature have been investigated. The products of the reactions have been characterized by dynamic light scattering (DLS) (hydrodynamic diameter and zeta potential) and thermogravimetric analyses (TGA). Indeed, the main goal was to obtain the smallest possible hydrodynamic diameter with the densest coating, which implied a maximum passivation of the surface (zeta-potential close to zero) and a high weight loss percentage by TGA. This weight loss percentage was determined between 150 and 550 °C, range in which only the organic part of the nanoparticles, i.e., the coating could degrade. An example of those analyses is shown (Fig. S2).

Finally, the best conditions for the functionalization with both polymers have been obtained using a 2/1 mass ratio in polymer/NPs in hydrochloric acid 5 mM (pH 2.5) at room temperature for 16 hours, as shown below (Fig. 2):

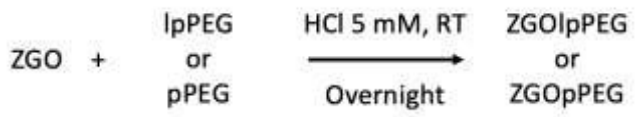

Figure 2: Optimized functionalization reaction of ZGO with lpPEG and pPEG.

After several centrifugations and washing with water, the obtained ZGOlpPEG and ZGOpPEG have been physico-chemically characterized (Fig. 3). First, the luminescence measured using a Biospace photon imager showed similar results for the three pegylated samples (figure 3A). In terms of size, ZGOpPEG present a small increase in hydrodynamic diameter (+ 30 nm), which is even smaller for the ZGOlpPEG (+ 20 nm), with a narrow size distribution (Fig. 3B). Both zeta potential and TGA confirmed the success of the functionalization (Fig. 3C). Zeta potential dropped for ZGOpPEG and ZGOlpPEG (- 2.5 and - 0.5 mV respectively) compared to ZGOOH (+ 15 mV) which show a good passivation of the surface charge. Similarly, TGA has shown high amount of coating for

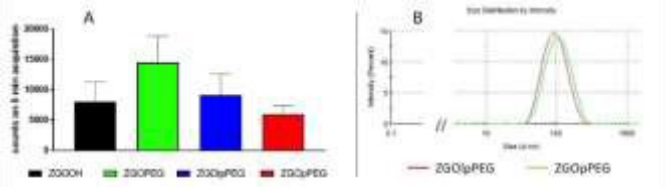

C

	ZGOOH	ZGOPEG	ZGOlpPEG	ZGOpPEG
HD (nm)	80 ± 7	145 ± 15	98 ± 2	109 ± 2
ζ – potential (mV)	14.5 ± 1.7	-2.5 ± 1.0	-0.5 ± 1.2	- 1.9 ± 0.3
TGA (w% coating)	1.4 %	6.5 %	5.7 %	8.6 %

Figure 3: Characterization of the different ZGO after functionalization. Luminescence properties after UV excitation (A) and size distribution of ZGOpPEG and ZGOlpPEG (B) were investigated. A summary of the different characterizations is presented in the table (C).

both ZGOpPEG (8.6 %) and ZGOlpPEG (5.7 %) compared to the ZGOOH control (1.4 %). Furthermore, the presence of grafted coating has been demonstrated using ^{31}P NMR on ZGOpPEG and ZGOlpPEG (Fig. S3, cf comments). The behavior of the newly coated NPs in biological fluids were then investigated to evaluate the possibility of their use for *in vivo* imaging.

Characterization in *in vivo* like media

Before injecting the NPs, their colloidal stability in the injection medium was investigated. Indeed, an aggregation on the injection site could lead to severe injuries by locally blocking the bloodstream, and therefore enabling the ZGO to circulate and to accumulate in the tissue of interest. To assess their stability in 5 % glucose, their hydrodynamic diameter as well as their polydispersity index have been recorded over the time (Fig. 4).

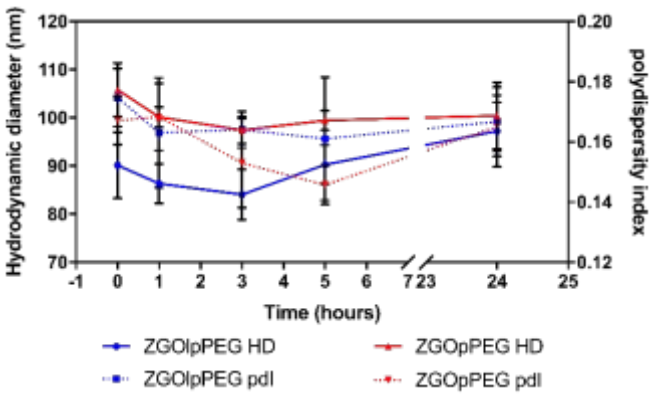

Figure 4: Evolution of the hydrodynamic diameter (continuous line) and polydispersity index (dashed line) of ZGOlpPEG (blue) and ZGOpPEG (red) in 5 % glucose injection medium (n=3).

The same behavior was observed for both ZGOlpPEG and ZGOpPEG. It first can be observed that NPs are stable in 5 % glucose with a mean diameter around 100 nm. It is interesting to notice that ZGOlpPEG shows larger variability than ZGOpPEG. This stability can be seen by looking at the evolution of the pdI. It stayed stable around 15% up to 24 h, which indicates no sign of aggregations. In any case, a viable stability of the NPs in the injection medium has been proven, and in vivo use can be considered.

After injection of the NPs into the bloodstream, the ZGO will be in contact with the plasma proteins. These proteins are likely to adsorb on the ZGO and therefore change their colloidal characteristics. To study these surface changes, the hydrodynamic diameter of the functionalized NPs, dispersed into mouse serum in 5% glucose (1/1 volume ratio), has been followed by DLS (Fig. 5).

The difference between the ZGOPEG and the two phosphonic acid-based PEG polymers is clear. While the ZGOPEG present a mean HD increase of 150 nm (100% increase) compared to the stock solution (Fig. 3C), a 50 nm increase is observed for ZGOpPEG (around 50%) and 80 nm for ZGOlpPEG (around 80%),

while the unfunctionalized ZGOOH present a 100 nm increase (125%). These observations indicate a clear limitation of the adsorption of plasma proteins on the surface of ZGOlpPEG and more especially on ZGOpPEG.[32] The colloidal stability of the NPs in mouse serum can also be assessed by looking at the evolution of the pdI over time. Expect for ZGOPEG, the pdI is proved to be constant up to 2 h, showing low variability. This observation is

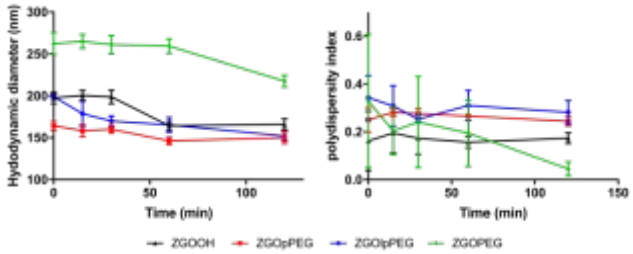

Figure 5: Evolution of the hydrodynamic diameter (left) and polydispersity index (right) of ZGOlpPEG (blue line), ZGOPEG (green line), ZGOOH (black line) and ZGOpPEG (red line) in diluted mouse serum in 5% glucose (n=3).

coherent with the low evolution of the HD observed before.
The quantification of adsorbed proteins can be obtained using a colorimetric Bradford test.[37] This test consists in incubating the NPs in serum for 2 h and to finally add the Bradford reacting agent, which changes the absorbance properties in contact with proteins. The concentration of adsorbed proteins on the NPs can then be quantified by using a calibration curve (Fig. S4). The results obtained for each surface chemistry is shown below (Fig. 6).The results exhibit significant differences between ZGOOH and both ZGOPEG, as already described,[22] and ZGOpPEG. The quantity of bound proteins per mg of ZGO is two-times lower (around 25 ng/mg) than for the unfunctionalized ZGO (around 50 ng/mg). ZGOlpPEG present a larger number of adsorbed proteins than ZGOOH. This result could be explained by the lower density of coating determined by TGA.

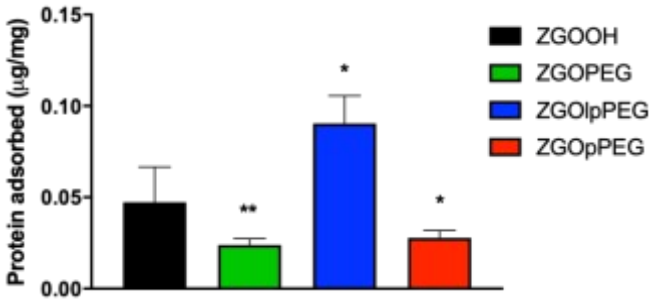

Figure 6: Bradford test showing the concentration of plasma proteins adsorbed on the surface of the different ZGO (n=5). Statistical differences with ZGOOH have been determined with the Mann-Whitney test (*: $p < 0.1$; **: $p < 0.01$).

Biodistribution study in mice

Each functionalized ZGO has been administrated to three healthy mice. Suspension of NPs at 10 mg/mL in 5 % glucose have been prepared and placed in a syringe. To excite the NPs, the syringes have been placed under a UV lamp for 1 min.

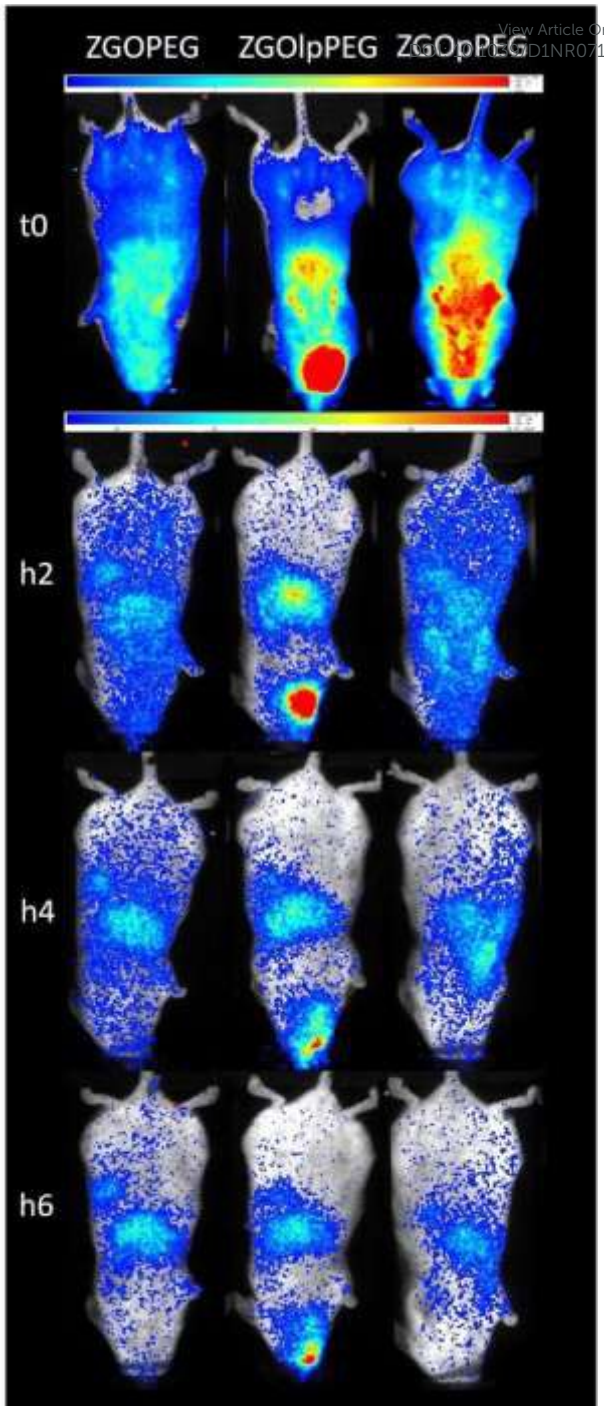

Figure7: Biodistribution of the differently coated nanoparticles in healthy mice. At t0 the luminescence was recorded after ex vivo UV excitation (scale 0.5-5) and then the signal was followed after in vivo visible light excitation (scale 0.05-0.5).

Finally, 0.2 mL of the suspension has been parenterally injected in retro-orbital site. The luminescence has been followed continuously during the first hour by repeated 10 min acquisition. Once the persistent luminescence signal became low, mice were re-excited for 2 min with a visible light before the different point measurements at longer times.
An overview of the biodistribution study is shown below (Fig. 7). The acquisition just after injection (T0) shows that both ZGOPEG and ZGOpPEG are well distributed inside the body. This can be

due the small HD variability in 5 % glucose (Fig. 4). Nevertheless, the amount of ZGOlpPEG going in the bloodstream seems to circulate. On the other hand, the ZGOpPEG present an intense signal coming from the upper part of the mice. The longer time point study exhibits a similar behavior: the maximum intensity for ZGOlpPEG is still coming from the injection site, while both ZGOPEG and ZGOpPEG circulate. An accumulation in the liver seems to occur 4 h after injection and is confirmed after 6 h. To sum up, we can affirm that ZGO have been successfully functionalized by pPEG and such NPs can circulate in the bloodstream freely for more than 4 h and seems to present the same furtivity than ZGOPEG.

To have a better understanding of the biodistribution, the mice were sacrificed 6 h after injection and the main organs (liver, lungs, kidneys, spleen, heart, and blood) were collected. *Ex vivo* excitation of the tissues was performed to detect more precisely the provenance of the luminescence signal (Fig. 7). As already described,[6] the ZGOPEG are essentially maintained in the liver and the spleen 6 h after injection likewise the ZGOlpPEG, as seen in the early time points. In any case, no luminescence signal was observed in the blood, suggesting a total clearance of the ZGO from the bloodstream. On the contrary, the ZGOpPEG does not present the same behavior. The recorded luminescence signal originates also from the liver and the spleen, but also distribute in the lungs and the kidneys. To quantify these observations, the luminescence signal coming from the tissues has been counted on a 5 min acquisition, and the resulting photon counts have been normalized by the mass of each organ (Fig. 8).

As observed before, the signal of luminescence in the liver is the same for the three NPs. The spleen also presents a large uptake of the ZGOs, because of its active role in the MPS. The observation made before are confirmed by the quantification. The ZGOpPEG are well present in the kidneys, the lungs and more surprisingly in the heart. These results suggests either a continuous circulation in the blood or new cellular interactions. Following these observations, ICP-MS quantifications of the zinc and gallium content in the organs have been performed. The obtained concentrations have been normalized in comparison to the initial injected dose (Fig. 9). As seen before, NPs are mainly present into the liver and spleen, but a larger percentage of ZGOpPEG is observed into the lungs and blood. This result is consistent with a longer circulation time into the bloodstream. On the other hand, a larger quantity of ZGOpPEG in the kidneys is also observed, which was already noted with *ex vivo* luminescence.

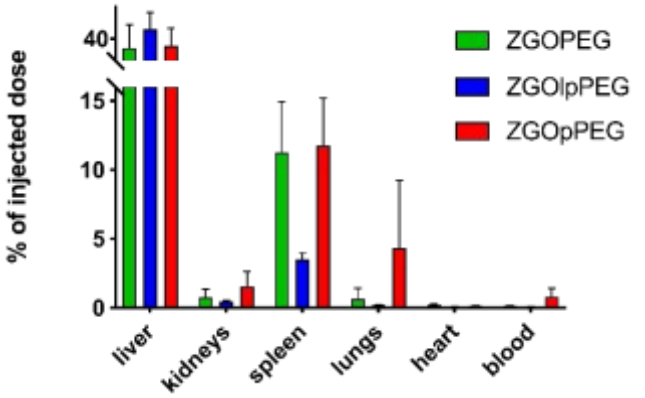

Figure 9: ICP-MS quantification of ZGO content in each organ depending on the coating. Results have been normalized in comparison with the initial injected dose.

From these results, we can see that the structure of the pPEG offers new possibilities. Because of the number of phosphonic acid anchor per polymer, it is unlikely that each one of them binds to the ZGO. Therefore, some of the anchor sites could be in direct interaction with the biological environment. The phosphonic acid have been investigated for their role in various biological processes and has been shown to be able to fix active binding sites, such as tyrosine phosphatases.[38] ZGOpPEG could link to different proteins or induce different interactions with cells in contrast to ZGOPEG. Therefore, new investigations could be envisioned such as the passive targeting of kidneys using ZGOpPEG.

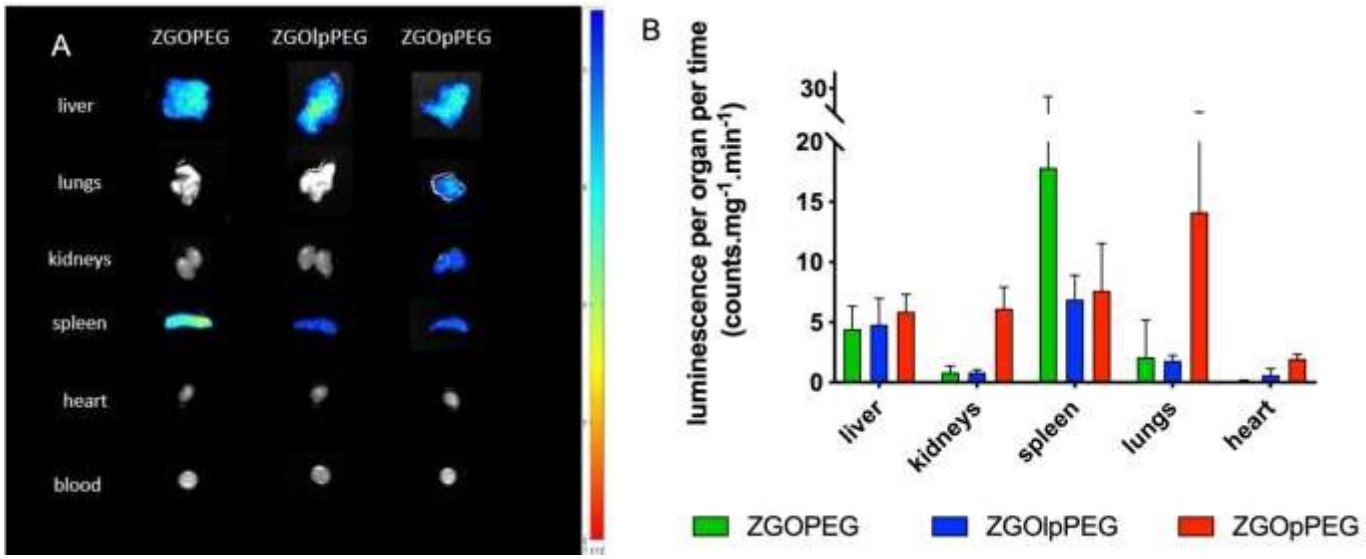

Figure 8: Ex vivo luminescence of the different organs 6 h after injection (left) and quantification of the luminescence signal after ex vivo visible light excitation (right).

Experimental

Chemicals were obtained from Sigma-Aldrich, Fluka or Alfa-Aesar. Alpha-methoxy-omega N-hydroxysuccinimide poly(ethylene glycol) PEG MW 5.000 Dalton was bought from Iris Biotech GmbH. Water refers to Millipore water.

Polymer synthesis

Synthesis of PEGMA$_{5k}$-MPh copolymer

Free radical polymerization of PEGMA$_{5k}$and MAPC1 ester with AIBN as radical initiator was performed leading to the targeted copolymer. The deprotection of phosphonated esters of the terpolymer was carried out in presence of bromotrimethylsilane ($BrSiMe_3$). Following this step, phosphonic acid was recovered. Final copolymer PEGMA$_{5k}$-MPh was obtained by precipitation in cold ether as a white powder. Synthesis pathway and NMR spectra are presented in Fig. S5.

Preparation of 1.

MAPC1 ester (1.25 g, 6.0 mmol), MPEG$_{5K}$ (30 g, 6.0 mmol), and AIBN (0.312 g, 1.9 mmol) were added along with 60 mL of methylethyl ketone (MEK) in a two-necked round-bottom flask. The mixture was heated at 70°C under argon in a thermostatic oil bath for 24 hours leading to 100 % conversion. Conversion was monitored by ^{1}H NMR spectroscopy. MEK was evaporated and the terpolymer was dissolved in a small volume of THF before precipitation in cold ether. A white powder (PEGMA$_{5k}$-MAPC1$_{ester}$) was obtained in 85 % yield.

^{1}H NMR (300 MHz, $CDCl_3$) δ (ppm): 4.49 – 3.91 (-C$\underline{H}_2$-O-C=O), 3.90 – 3.27 (-O-C$\underline{H}_2$-C$\underline{H}_2$-O),3.8 – 3.91 O=P-(OC$\underline{H}_3$)$_2$), 3.22 (-CH$_2$-O-C$\underline{H}_3$), 2.8 – 0.8 (C(C$\underline{H}_3$)-C$\underline{H}_2$).

^{31}P NMR ($CDCl_3$, 300 MHz) δ (ppm): 21.7 (O=$\underline{P}$-(OCH$_3$)$_2$).

Preparation of 2.

Previously obtained copolymer (**PEGMA$_{5k}$-MAPC1$_{ester}$**, 22.2g) was dissolved in a minimum of dichloromethane (100 mL) and degassed with argon. Bromotrimethylsilane (3.7 g, 24 mmol) was added dropwise to the reactive media under inert and dry conditions. The solution was stirred for 8 hours, then the solvent was removed with a rotatory evaporator. Ethanol was then added in excess (30 mL) to complete ethanolysis. Finally, targeted terpolymer was precipitated in cold ether leading to the PEGMA$_{5k}$-MPh final product in 81 % yield.

^{1}H NMR (300 MHz, $CDCl_3$) δ (ppm): 4.33 – 3.27 (C$\underline{H}_2$-O-C=O, C$\underline{H}_2$-C$\underline{H}_2$-O), 3.23 (CH$_2$-O-C$\underline{H}_3$), 2.5 – 0.8 (C(C$\underline{H}_3$)-C$\underline{H}_2$).

^{31}P NMR ($CDCl_3$, 300 MHz) δ (ppm): 18.6 (O=$\underline{P}$-(OH)$_2$).

Synthesis of PEG5K-Ph

The phosphonic group is introduced by radical addition of diethylphosphite on allyl function of the allyl-PEG in presence of AIBN. Phosphonic acid 4 is obtained by deprotection of phosphonate group with the $BrSiMe_3$. The monomer 4 is then obtained by precipitation in cold ether as white powder. A representative synthesis leading to PEG$_{5k}$-Ph is presented with detailed NMR spectrum in Fig. S6.

Preparation of 3.

In a two-necked round-bottom flask was introduced vinyl-PEG (10 g, 1.98 mmol), Diethyl phosphite (5.5 g, 39.7 mmol, 20 eq), the solution is heated at 110°C. tert butyl Peroxypivalate (23mg, 9.92 10^{-2} mmol) was added dropwise to the reactive media. The reaction is let at 110°C for half an hour, then diethyl phosphite is evaporated. The mixture is solubilized in a minimum of dichloromethane to be precipitated in cold ether. The powder is filtrated to obtained white powder, PEG5K-Ph ester. (8.9 g, 83 % yield)

^{1}H NMR (300 MHz, D_2O) δ (ppm): 4.17 – 4.02 ((O=P-C$\underline{H}_2$-CH$_3$)$_2$), 3.76 – 3.51 (-O-C$\underline{H}_2$-C$\underline{H}_2$-O), 3.37 (-O-CH$_2$-CH$_2$-O-C$\underline{H}_3$), 1.75 – 1.95 (-O-C$\underline{H}_2$-C$\underline{H}_2$-P=O),1.31 ((O=P-CH$_2$-C$\underline{H}_3$)$_2$.

^{31}P NMR (D_2O, 300 MHz) δ (ppm): 32.3 (O=$\underline{P}$-(O-CH$_2$-CH$_3$)$_2$).

Preparation of 4.

Previously obtained polymer (PEG5K-Ph ester, 5 g, 0,97 mmol) was dissolved in a minimum of dichloromethane (30 mL) and degassed with argon. Bromotrimethylsilane (0.31 g, 2 mmol, 2.1 eq) was added dropwise to the reactive media under inert and dry conditions. The solution was stirred 8 hours, then the solvent was removed with a rotatory evaporator. Ethanol (30 mL) was then added in excess to complete ethanolysis. Finally, targeted terpolymer was precipitated in cold ether leading to 4.4 g of PEG5K-Ph final product in 88 % yield.

^{1}H NMR (300 MHz, D_2O) δ (ppm): 3.48 – 3.80 (-O-C$\underline{H}_2$-C$\underline{H}_2$-O), 3.33 (-O-CH$_2$-CH$_2$-O-C$\underline{H}_3$), 1.64-1.88 (-O-C$\underline{H}_2$-C$\underline{H}_2$-P=O).

^{31}P NMR (D_2O, 300 MHz) δ (ppm): 29.45 (O=$\underline{P}$-(OH)$_2$).

ZGO synthesis

$ZnGa_2O_4$:Cr^{3+} nanoparticles were synthesized by the hydrothermal developed in our lab. First, gallium nitrate was formed by reacting 8.94 mmol of gallium oxide with 20 mL concentrated nitric acid (35 wt %) under hydrothermal condition at 150°C for 24 hours. Then, a mixture of 0.04 mmol of chromium nitrate and 8.97 mmol of zinc nitrate in 10 mL of water was added to the previous solution of gallium nitrate under vigorous stirring. The resulting solution was adjusted to pH 7.5 with an ammonia solution (30 wt %), stirred for 3 hours at room temperature, and transferred into a 45 mL Teflon-lined stainless-steel autoclave for 24 h at 120°C. The resulting compound was washed several times with water and ethanol before drying at 60°C for 2 hours. The dry white powder was finally sintered in air at 750°C for 5 hours. Hydroxylation was performed by basic wet grinding of the powder (500 mg) for 15 minutes, with a mortar and pestle in 2 mL of 5 mM HCl solution, and vigorously stirred overnight at room temperature at 10 mg/mL in 5 mM HCl. Nanoparticles with a diameter of 80 nm were first selected from the whole polydisperse colloidal suspension by centrifugation (SANYO MSE Mistral 1000 at 4500 rpm for 10 minutes) and collected in the supernatant (assessed by Dynamic Light Scattering). The supernatants were gathered and concentrated to obtain the final ZGOOH stock suspension.

Preparation of PEG-coated nanoparticles (silane two-steps strategy)

The PEGylation of ZGOOH nanoparticles was performed by a two-step synthesis already described in the literature. 5 5 mg of

ZGOOH are washed with water and twice with DMF before being suspended in 2 mL of DMF. After addition of 20 µL of (3-aminopropyl)triethoxysilane (APTES), the solution was briefly sonicated and left stirring during 6 hours at ambient temperature. The resulting particles were washed twice with DMF and resuspended in 2 mL of DMF. 50 mg of NHS- activated PEG (MeO-PEG5kDa-NHS) were added and the solution is left stirring overnight at 90°C then washed twice with DMF before drying.

Preparation of lpPEG and pPEG-coated nanoparticles

Typically, 5 mg of ZGOOH were washed with HCl 5mM and placed in a round bottom flask at 1 mg/mL. Then, 10 mg of the corresponding polymer was added, and the mixture was briefly sonicated. The reaction took place overnight with vigorous stirring. The obtained functionalized NPs were then washed with water.

Nanoparticle's characterizations

Luminescence aquisition

5 minutes acquisitions of the luminescence of nanoparticles were recorded on an Optima (Biospace) camera after a 1-minute excitation under UV light (365nm) or under a LED lamp with a 515 nm filter. DLS and ζ-potential measurements in 20 mM NaCl were obtained with a Zetasizer Nano ZS (Malvern Instruments). TGA was conducted on a TGA/DSC 1 (Mettler Toledo S.A) between 25°C and 800°C (ramp: 10°C/min), and the weight loss percentage was estimated between 150°C and 550°C.

Stability of nanoparticles in different media

The hydrodynamic diameter of the differently functionalized ZGO (2 mg/mL suspensions in different media) was followed by DLS. Media used are 5 % glucose and 50 % mice serum in 5 % glucose solution.

Quantification of adsorbed proteins through Bradford assay

The commercial solution was diluted 5 times and filtered with a 0.22 µm filter. ZGO are incubated at a 2 mg/mL concentration in 50 % mice serum in 5 % glucose at 37°C for 2 hours. Nanoparticles were washed from unbound proteins by several centrifugation steps (13 400 rpm for 15 minutes at room temperature). Absence of unbound proteins in the last supernatant is verified with a Bradford assay. 10 µL of a 1 mg/mL suspension of washed nanoparticles in 5 % glucose were transferred to a 96-well plate (6 wells per sample). Next, 200 µL of Coomassie blue dye reagent (Bio-Rad) was added to each well, and the plate was incubated at 37°C for 10 minutes. Absorbance at 595 nm was measured using a plate reader (Tecan Infinite F200 Pro).

In vivo biodistribution studies

All experiments involving mice were approved by French *Comité d'éthique en expérimentation animale* N°034 and by French Ministry of Research APAFIS #8519-20 16090514387844.

***In vivo* and *ex vivo* luminescence signal acquisition**

10 mg of dried ZGOlpPEG, ZGOpPEG and ZGO-PEG were redispersed in 1 mL 5 % glucose. 200 µL (equivalent to 2 mg of nanoparticles) were collected with a syringe and excited during 2 minutes under a 365 nm UV lamp. Three mice are chemically anesthetized with isoflurane gas. The nanoparticles were then injected intravenously in the retro orbital area. During reexcitation and acquisition with Optima (Biospace) camera, mice are placed on their back and kept asleep with isoflurane. Luminescence is acquired with an Optima camera (Biospace) at different post-injection times for 10 minutes. For acquisition times longer than 1 hour after injection, nanoparticles are re-excited during 2 minutes under a LED (> 515 nm lamp) before acquisition. After 6 h, the mice have been sacrificed and the organs have been collected, rinsed with mQ water, and placed on black plate. The tissues have been excited 2 min with visible light. The count of luminescence has been performed exactly 1 min after the end of the excitation, on a 5 min acquisition time. The results have then been normalized by the corresponding mass of tissue.

ICP quantification

Organ samples kept at -80°C were thawed and then weighed directly from the tube. The different samples were put in the presence of 5 mL of distilled concentrated nitric acid (70%) for 24 h at 90°C using a Analab mineralization device. The solution was then allowed to cool, and the acid was diluted by adding 45 mL of mQ water. 50 µL of the solution were then taken and placed in 4.95 mL of mQ water for ^{66}Zn and ^{69}Ga analysis with the HR-ICP-MS Element II from ThermoScientific (PARI platform).

Conclusions

A new functionalization strategy has been developed using statistical copolymers bearing PEG lateral chains and multi phosphonic acids anchoring groups. The coating has been optimized, and good colloidal stability has been obtained in injection medium. The incubation of ZGOpPEG in mouse serum has exhibited a low adsorption of plasma proteins confirmed by both DLS and Bradford test. Finally, the biodistribution study in mice has shown a circulation time in blood for more than 4 h, comparable to the ZGOPEG. Furthermore, differences in organs biodistribution have been reported.

Finally, in this work we have developed a one-step reaction in aqueous medium with a lower amount of polymer used, a higher coating density, a controlled size distribution, while observing long circulation time after injection in the bloodstream. This allows us to consider new potentials for these ZGO NPs as well as new targeting strategies. Furthermore, this new functionalization strategy, only realized in aqueous medium, is a much safer alternative for *in vivo* studies.

Author Contributions

T. Lécuyer was the principal contributor on the experimental work. N. Bias oversaw the polymers' synthesis, under the supervision of A. Graillot and C. Loubat. J. Seguin brought expertise with *in vivo* imaging and Y. Corvis with thermogravimetric analysis. J. Liu helped with the synthesis of

View Article Online
DOI: 10.1039/D1NR07114A

ZGO and L. Valero with DLS analysis. P. Burckel oversaw the ICP-MS measurements. Finally, D. Scherman, N. Mignet and C. Richard oversaw this work and brought fundings to support this study.

Conflicts of interest

There are no conflicts to declare.

Acknowledgements

This work was supported by French research agency (ANR-14-CE08-0016-01). Authors would like to thank the PARI platform for ICP-MS measurement, and the LIOPA platform for the *in vivo* imaging. Authors would like to thank M. Ilyess Zouaoui for the graphical work.

Notes and references

1 S. H. Yun and S. J. J. Kwok, *Nat. Biomed. Eng.*, 2017, **1**, 0008.

2 J. V. Frangioni, *Curr. Opin. Chem. Biol.*, 2003, **7**, 626–634.

3 S. Bouccara, G. Sitbon, A. Fragola, V. Loriette, N. Lequeux and T. Pons, *Curr. Opin. Biotechnol.*, 2015, **34**, 65–72.

4 T. Lécuyer, E. Teston, G. Ramirez-Garcia, T. Maldiney, B. Viana, J. Seguin, N. Mignet, D. Scherman and C. Richard, *Theranostics*, 2016, **6**, 2488–2524.

5 J. P. M. Almeida, A. L. Chen, A. Foster and R. Drezek, *Nanomed.*, 2011, **6**, 815–835.

6 J. Key and J. F. Leary, *Int. J. Nanomedicine*, 2014, **9**, 711–726.

7 T. Maldiney, A. Bessière, J. Seguin, E. Teston, S. K. Sharma, B. Viana, A. J. J. Bos, P. Dorenbos, M. Bessodes, D. Gourier, D. Scherman and C. Richard, *Nat. Mater.*, 2014, **13**, 418–426.

8 J. Liu, T. Lécuyer, J. Seguin, N. Mignet, D. Scherman, B. Viana and C. Richard, *Adv. Drug Deliv. Rev.*, , DOI:10.1016/j.addr.2018.10.015.

9 T. Maldiney, M. U. Kaikkonen, J. Seguin, Q. le Masne de Chermont, M. Bessodes, K. J. Airenne, S. Ylä-Herttuala, D. Scherman and C. Richard, *Bioconjug. Chem.*, 2012, **23**, 472–478.

10 G. Ramírez-García, S. Gutiérrez-Granados, M. A. Gallegos-Corona, L. Palma-Tirado, F. d'Orlyé, A. Varenne, N. Mignet, C. Richard and M. Martínez-Alfaro, *Int. J. Pharm.*, 2017, **532**, 686–695.

11 I. Sekler, S. L. Sensi, M. Hershfinkel and W. F. Silverman, *Mol. Med.*, 2007, **13**, 337–343.

12 S. Choi, B. E. Britigan and P. Narayanasamy, *Antimicrob. Agents Chemother.*, 2017, **61**, e02505-16.

13 S. Terpilowska and A. K. Siwicki, *Chemosphere*, 2018, **201**, 780–789.

14 Y. Jiang, Y. Li, C. Richard, D. Scherman and Y. Liu, *J. Mater. Chem. B*, 2019, **7**, 3796–3803.

15 T. Lécuyer, M.-A. Durand, J. Volatron, M. Desmau, R. Lai-Kuen, Y. Corvis, J. Seguin, G. Wang, D. Alloyeau, D. Scherman, N. Mignet, F. Gazeau and C. Richard, *Nanoscale*, 2020, **12**, 1967–1974.

16 E. Teston, T. Maldiney, I. Marangon, J. Volatron, Y. Lalatonne, L. Motte, C. Boisson-Vidal, G. Autret, O. Clément, D. Scherman, F. Gazeau and C. Richard, *Small*, 2018, **14**, 1800020.

17 H. Liu, H. Yin, T. Yang, H. Ding and Y. Dong, *Analyst*, 2020, **145**, 7412–7420.

18 M. Hofmann-Amtenbrink, D. W. Grainger and H. Hofmann, *Nanomedicine Nanotechnol. Biol. Med.*, 2015, **11**, 1689–1694.

19 V. Pareek, A. Bhargava, V. Bhanot, R. Gupta, N. Jain and J. Panwar, *J. Nanosci. Nanotechnol.*, 2018, **18**, 6653–6670.

20 J. Li, X. Chang, X. Chen, Z. Gu, F. Zhao, Z. Chai and Y. Zhao, *Biotechnol. Adv.*, 2014, **32**, 727–743.

21 M. Zhu, G. Nie, H. Meng, T. Xia, A. Nel and Y. Zhao, *Acc. Chem. Res.*, 2013, **46**, 622–631.

22 T. Maldiney, M. Rémond, M. Bessodes, D. Scherman and C. Richard, *J. Mater. Chem. B*, 2015, **3**, 4009–4016.

23 K. Knop, R. Hoogenboom, D. Fischer and U. S. Schubert, *Angew. Chem. Int. Ed Engl.*, 2010, **49**, 6288–6308.

24 L. Fu, J. Wang, N. Chen, Q. Ma, D. Lu and Q. Yuan, *Chem. Commun.*, 2020, **56**, 6660–6663.

25 A. Li, H. P. Luehmann, G. Sun, S. Samarajeewa, J. Zou, S. Zhang, F. Zhang, M. J. Welch, Y. Liu and K. L. Wooley, *ACS Nano*, 2012, **6**, 8970–8982.

26 V. Baldim, N. Bia, A. Graillot, C. Loubat and J. Berret, *Adv. Mater. Interfaces*, 2019, **6**, 1801814.

27 J.-M. Rueff, M. Poienar, A. Guesdon, C. Martin, A. Maignan and P.-A. Jaffres, *J. Solid State Chem.*, 2016, **236**, 236.

28 R. Gomes, A. Hassinen, A. Szczygiel, Q. Zhao, A. Vantomme, J. C. Martins and Z. Hens, *J. Phys. Chem. Lett.*, 2011, **2**, 145–152.

29 G. Ramniceanu, B.-T. Doan, C. Vezignol, A. Graillot, C. Loubat, N. Mignet and J.-F. Berret, *RSC Adv.*, 2016, **6**, 63788–63800.

30 R. Li, Z. Ji, J. Dong, C. H. Chang, X. Wang, B. Sun, M. Wang, Y.-P. Liao, J. I. Zink, A. E. Nel and T. Xia, *ACS Nano*, 2015, **9**, 3293–3306.

31 J. L. Braid, U. Koldemir, A. Sellinger, R. T. Collins, T. E. Furtak and

View Article Online
DOI: 10.1039/D1NR07114A

D. C. Olson, *ACS Appl. Mater. Interfaces*, 2014, **6**, 19229–19234.

32 V. Torrisi, A. Graillot, L. Vitorazi, Q. Crouzet, G. Marletta, C. Loubat and J.-F. Berret, *Biomacromolecules*, 2014, **15**, 3171–3179.

33 C. M. Sevrain, M. Berchel, H. Couthon and P.-A. Jaffrès, *Beilstein J. Org. Chem.*, 2017, **13**, 2186–2213.

34 L. D. Freedman and G. O. Doak, *Chem. Rev.*, 1957, **57**, 479–523.

35 M. Montalti, S. Wadhwa, W. Y. Kim, R. A. Kipp and R. H. Schmehl, *Inorg. Chem.*, 2000, **39**, 76–84.

36 A. Graillot, D. Bouyer, S. Monge, J.-J. Robin, P. Loison and C. Faur, *J. Hazard. Mater.*, 2013, **260**, 425–433.

37 M. M. Bradford, *Anal. Biochem.*, 1976, **72**, 248–254.

38 E. M. B. Fonseca, D. B. B. Trivella, V. Scorsato, M. P. Dias, N. L. Bazzo, K. R. Mandapati, F. L. de Oliveira, C. V. Ferreira-Halder, R. A. Pilli, P. C. M. L. Miranda and R. Aparicio, *Bioorg. Med. Chem.*, 2015, **23**, 4462–4471.